Molecular Crystals and Liquid Crystals
Publication details, including instructions for authors and subscription information:
http://www.tandfonline.com/loi/gmcl16

# Dynamical Study of Heat Conduction in Liquid Crystals by High-Speed Optical Holography

S. Kuroda [a] , M. Kimura [a] & K. Kubotoa [a]
[a] Faculty of Science, Kwansei Gakuin University, Nishinomiya, Japan
Version of record first published: 28 Mar 2007.

To cite this article: S. Kuroda , M. Kimura & K. Kubotoa (1976): Dynamical Study of Heat Conduction in Liquid Crystals by High-Speed Optical Holography, Molecular Crystals and Liquid Crystals, 33:3-4, 235-246

To link to this article: http://dx.doi.org/10.1080/15421407608084299

*Mol. Cryst. Liq. Cryst.*, 1976. Vol. 33, pp.235–246

Printed in Holland



# Dynamical Study of Heat Conduction in Liquid Crystals by High-Speed Optical Holography

S. KURODA, M. KIMURA and K. KUBOTA

*Faculty of Science, Kwansei Gakuin University, Nishinomiya, Japan*

(*Received March 31, 1975; in final form October 20, 1975*)

We applied high-speed optical holography to the study of the mesophase-isotropic phase transition of liquid crystals. We generated a small thermal disturbance at a point in a liquid crystal by means of a cw laser beam. We then followed the changes of the refractive index in space and time by using double-exposure optical holography with pulsed laser light. We measured the thermal diffusivity by changing the sample temperature in the isotropic phase. Anomalous behaviour of thermal conduction was observed near the transition point. The samples studied were *p*-methoxybenzylidene *p*-*n*-butylaniline (MBBA) and cholesteryl pelargonate. We analyzed the experimental results by using hydrodynamic equations, and discussed the contribution of the short-range order effect.

## 1 INTRODUCTION

It is known that a first-order phase transition occurs in a liquid crystal at the transition temperature, $T_C$ (mesophase-isotropic phase transition). The isotropic phase shows some short-range order effects slightly above $T_C$. Litster and Stinson reported anomalous magnetic birefringence and scattering of light by *p*-methoxybenzylidene *p*-*n*-butylaniline (MBBA).[1,2] Recently de Gennes introduced the tensor order parameter $Q$ and explained the experimental results from the standpoint of the short-range order.[3]

In the work reported in this present article we have measured the temperature dependence of the thermal conductivity in the isotropic phase and we have given special attention to the behaviour near the phase transition. In our experiments we generated a small thermal disturbance at a point in a liquid crystal and followed the changes of the refractive index in space and time by means of double-exposure optical holography. The samples studied were a nematic (MBBA) and a cholesteric (cholesteryl pelargonate) liquid

crystal. We obtained anomalous thermal conduction near the transition temperature, and considered the effect of the short-range order on this phenomenon.



## 2 EXPERIMENTAL ARRANGEMENT

A schematic diagram of the experimental arrangement is shown in Figure 1. A Q-switched ruby laser was used as the light source for high-speed holography. The laser beam was split by the mirror $M_1$, reflected by the mirrors $M_2$, $M_3$ and $M_4$, and superimposed on the holographic film. The pinhole between lenses improved the coherence of the laser light. Samples were MBBA and cholesteryl pelargonate. The sample cell of thickness 1–3 mm was placed in one of the optical paths of the laser beam. The cell temperature was controlled to be constant $\pm 0.05°$ in the range between 40°C and 90°C before the application of a small thermal disturbance. We used the cw argon laser to heat a small point in the sample. The argon laser beam irradiated the sample through the mirror $M_3$. Heating by an optical beam has the following merits;

1) it gives a short rectangular pulse of heat
2) it generates heat in a spot region without any contact of heating wires

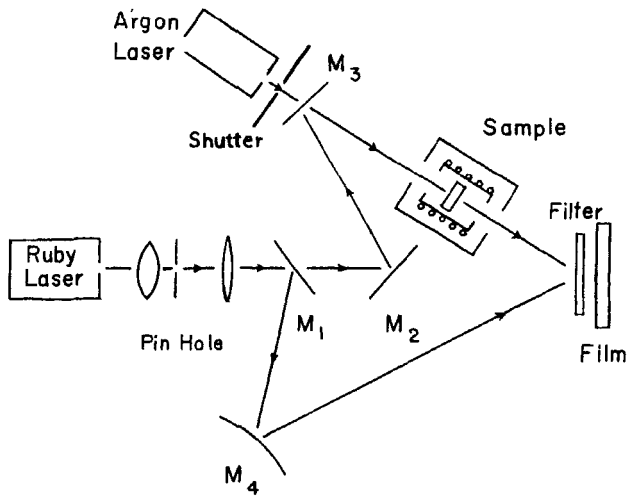


FIGURE 1 Experimental arrangement. The mirror $M_1$ splits the ruby laser beam. The Ar laser beam irradiates the sample through the mirror $M_3$. A pinhole is for improving the coherence of the ruby laser light. The filter transmits the ruby laser beam only. The shutter is for switching on the Ar laser beam.

3) it is possible to study transport phenomena without any obstacle to the material flow.

## 3 EXPERIMENTAL RESULTS

The double-exposure holography was performed in the following way; the first exposure was made without irradiation by the argon laser beam and the second was made with irradiation. The exposure time was defined as the time interval between switching on the Ar laser and the second exposure by the ruby laser. The refractive index change recorded on the hologram was due to the heat produced by the Ar laser beam during the exposure time. The interference fringes in the reconstructed image of the hologram correspond to the isorefractive index lines in the sample. There were several concentric-circular fringes around the Ar laser beam, which are shown in Figure 2. We derived from Figure 2 the spatial distribution of the change in refractive index, $n_1$, in the sample. The coherence length of the ruby laser used in our experiments limited the spatial resolution to, at most, $5 \times 10^{-2}$ mm. Figure 3 gives the results at various exposure times, $t$, for MBBA. The refractive index at the innermost fringe near the center of the sample was calculated from the known refractive index at the outermost fringe. In our

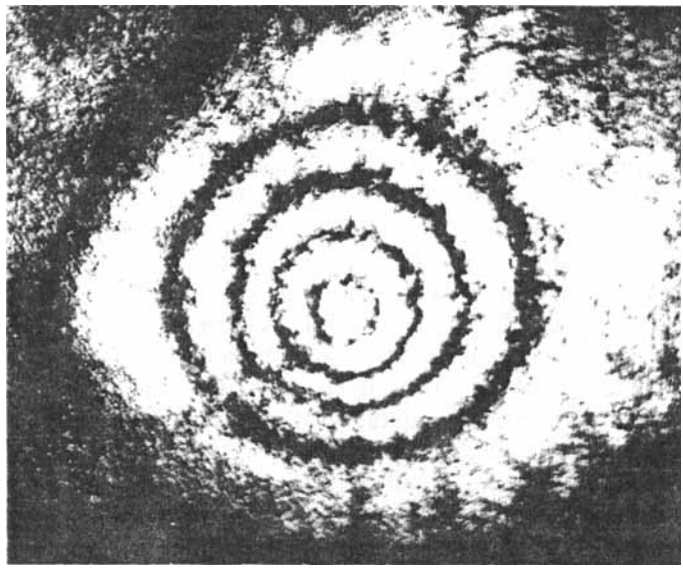

FIGURE 2 Reconstructed image from a double-exposed hologram. Concentric circles correspond to the isorefractive index lines.

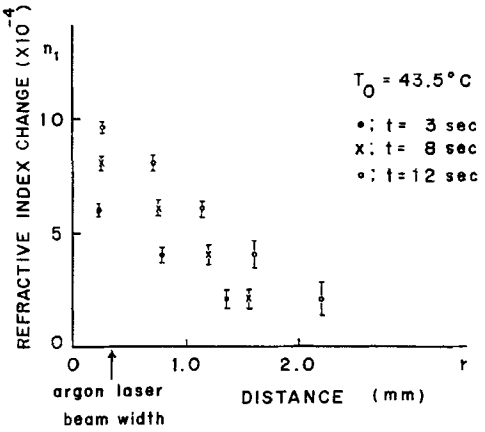


FIGURE 3 Spatial distribution of the refractive index change in MBBA at various exposure times of the Ar laser beam.

experiments the difference between these two values was of order $10^{-4}$ and the temperature increase at the center was very small.

The refractive index outside the outermost fringe was equal to the known value at the initial, undisturbed, temperature of the liquid crystal, which was measured by the thermocouple of the temperature-control system. This thermocouple was in contact with the wall of the cell and gave the temperature near the surface of the liquid crystal sample, which was, before the generation of the thermal disturbance, constant throughout the whole sample. Because this thermocouple was at the wall of the cell, the time interval between the initiation of the thermal disturbance and the second ruby-laser exposure was limited to the time interval required for the outermost fringe to reach the wall of the cell where the constant temperature, $T_0$, was being maintained. Measurement of the value of the refractive index of the liquid crystal at temperature $T_0$ thus permitted us to know its value at the outermost fringe and hence the change in its value between the innermost and outermost fringes. Figure 4 shows the $T_0$-dependence of $n_{10}$, where $n_{10}$ is the value of $n_1$ at the center which was obtained by extrapolation of the plots in Figure 3. Near the transition temperature $T_C$ (41.8°C) $n_{10}$ decreased abruptly, especially when the duration of Ar laser irradiation was short. Since the exposure time was of the order of 1 sec and the energy density of the ruby laser in the cell was small compared with that of the Ar laser beam, the effect of the ruby laser light on the thermal disturbance was neglected.

We performed the same experiment for cholesteryl pelargonate ($T_C$ = 86.0°C). The result is shown in Figure 5. It seems that the heat conduction in cholesteryl pelargonate is slow near $T_C$ compared with that of MBBA.

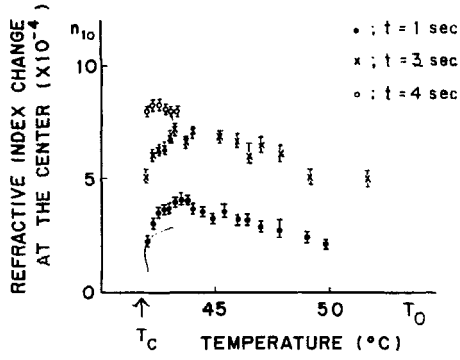


FIGURE 4 Plots of the refractive index change at the center of the Ar laser beam in MBBA for the cell temperature. Anomalous behaviour is observed near the transition temperature for the exposure times within 3 sec.

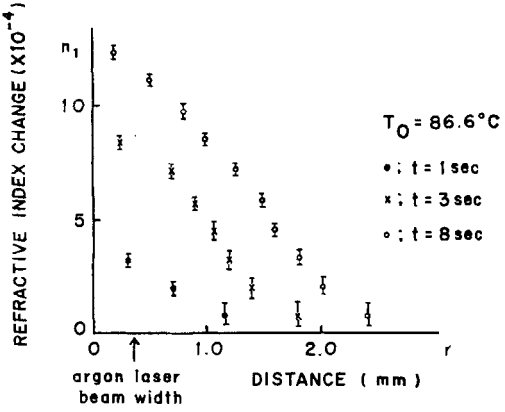


FIGURE 5 Spatial distribution of the refractive index change in Cholesteryl pelargonate at various exposure times.

On the other hand, when the intense optical beam passes through the absorbing material, the outgoing beam spreads; this is called the self-defocusing effect.[4] The Ar laser pattern on the screen behind the cell is shown in Figure 6. From this figure we calculated the refractive index of the material. The calculated value was of the same order of magnitude as that obtained from the holographic method. When irradiation of the Ar laser continued for a long time (more than several tens of seconds), a macroscopic large convection of the fluid occurred in the sample. Then, both patterns of the self-defocusing and the reconstructed fringe of the hologram deformed remarkably. Figure 7 is a reconstructed image from the hologram. The sample was irradiated by the 800 mw Ar laser beam for a few minutes.

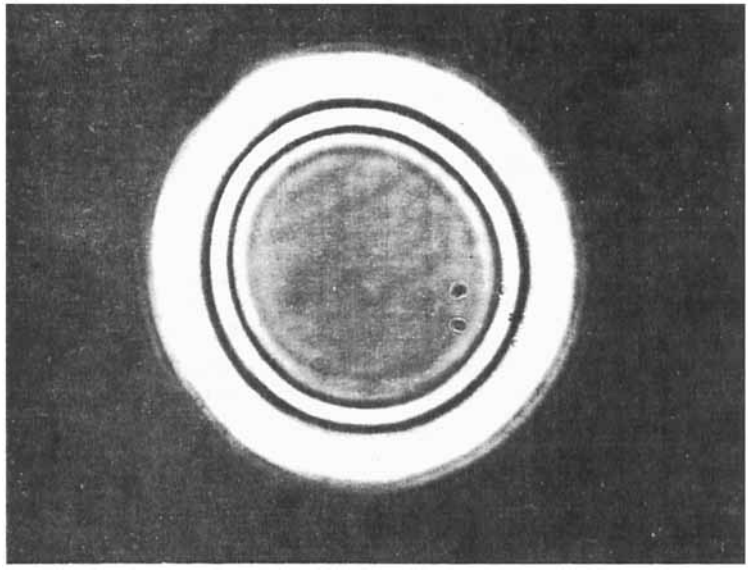

FIGURE 6 Self-defocusing pattern of the Ar laser beam passing through the MBBA cell.

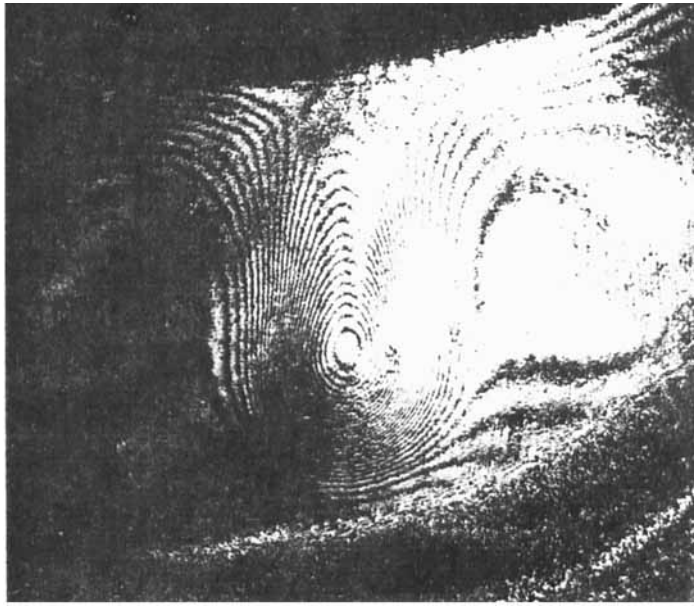

FIGURE 7 Reconstructed image from a double-exposed hologram. The sample is irradiated by the 800 mw Ar laser beam for a few minutes. Isorefractive index lines show the convection in the sample.

## 4 THEORY

The heat given by the Ar laser beam diffuses in the liquid, and a temperature gradient is generated. The thermal gradient produces a change in the spatial distribution of the refractive index. We discuss this problem by using an equation of heat conduction. Since the perturbation is very small, we treat the linearized equation of motion;

$$\rho_0 C_V \frac{\partial T_1}{\partial t} - K\nabla^2 T_1 = J, \tag{1}$$

where $\rho_0$ is the density of the liquid crystal, $C_V$ is the specific heat at constant volume, $T_1$ is the temperature change and $J$ is the external heating rate per unit volume. Here we assume that in the small temperature region around $T_C$ the conductivity $K$ depends on the original temperature $T_0$.

We represent the intensity distribution of the Ar laser beam as

$$P(r) = P_{10}(1 - A^2r^2)\exp(-A^2r^2), \tag{2}$$

where $P_{10}$ is the optical power at the center of the beam, $r$ is the distance from the beam center and $1/A$ is the beam radius.

Using Eq. 2, we describe $J$ as

$$J = 0.24\alpha P_{10}(1 - A^2r^2)\exp(-A^2r^2), \tag{3}$$

where $\alpha$ is the absorption coefficient of the Ar laser beam.

Equation 1 is solved with Eq. 3. We assume axial symmetry and notice the behaviour in the vicinity of the Ar laser beam. The result obtained for the temperature distribution is

$$T_1 \simeq \frac{0.12\alpha P_{10} t}{\rho_0 C_V(1 + 4A^2Dt)}\left[1 - \frac{(2 + 4A^2Dt)A^2r^2}{1 + 4A^2Dt}\right], \tag{4}$$

where $D = K/(\rho_0 C_V)$ is the temperature-dependent diffusivity. The Ar laser is switched on at the time $t = 0$.

The temperature dependence of the refractive index at the wavelength of the ruby laser in the isotropic phase of MBBA is given by the following linear relation;

$$n = 1.5950 - 0.1515\frac{T - T_C}{T_C}. \tag{5}$$

The refractive index change of the order of $10^{-4}$ in our experiments corresponds to a temperature increase of $10^{-3}$ deg. Since the fluctuation is very small, it is assumed that the refractive index change $n_1$ is proportional to

$T_1$. From Eqs. 4 and 5, the time dependence of refractive index at the center is

$$n_{10} = \frac{ct}{1 + 4A^2Dt}, \tag{6}$$

where $c$ is a proportionality constant.

## 5 DISCUSSION

Figure 4 shows the critical behaviour of the refractive index near the transition temperature $T_C$ when the exposure time $t$ was short ($\lesssim 3$ sec). Figure 8 shows plots of $n_{10}$ for $t$ in this region. They are described by Eq. 6. In Figure 9 we show the temperature dependence of $D$ which is determined from a least-squares fit to the experimental data. We take $1/A = 0.4$ mm. In an ordinary liquid the diffusivity increases with increasing temperature. The liquid crystal also acts as an ordinary liquid above the transition point. We represent the thermal diffusivity $D$ as $D_0 + D_1$, where $D_1$ is effective near $T_C$ only. Figure 9 shows that $D_0$ is proportional to $(constant - T^{-1})$ between 44°C and 50°C when the unit of temperature $T$ is expressed on the Kelvin scale. Assuming that this behaviour can be extrapolated to temperatures below 44°C, we obtain the temperature dependence of $D_1 = D - D_0$;

$$D_1 \propto (T - T^*)^{-3/2}, \tag{7}$$

when $T^*$ is chosen as 41.0°C ($T \simeq T_0$).

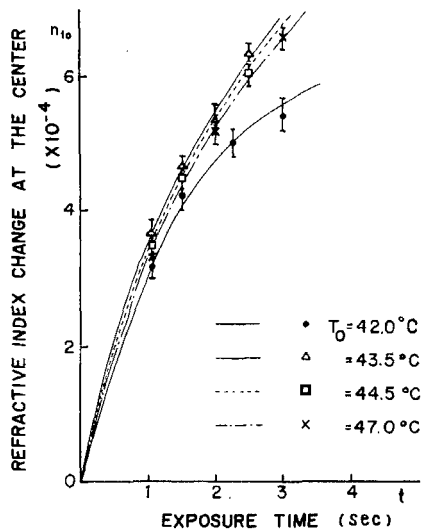


FIGURE 8 Plots of the refractive index change at the center in MBBA for the exposure times of the Ar laser beam. The curves are described by Eq. 6.

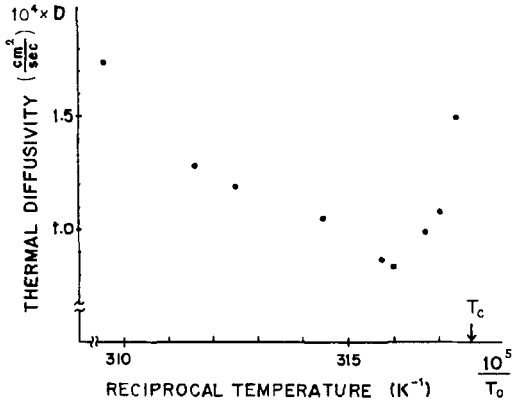


FIGURE 9 Temperature dependence of the diffusivity for MBBA. This is determined from a least-squares fit to the experimental data in Figure 8. Temperature is expressed on the Kelvin scale.

It is clear that the behaviour of $D$ near $T_C$ is closely related to the phase transition phenomenon. Fisher *et al.* studied the thermal conductivity of *p*-azoxyanisole (PAA) in the nematic phase.[5] It was shown that the molecular orientation of PAA had an influence on the thermal conductivity. Here we assume that the molecular ordering in the isotropic phase also contributes to the thermal conduction. Consideration of the relation between the short-range order parameter $Q$ and the thermal conductivity is given in the Appendix. Comparing Eq. 7 with Eq. A8 and taking $T_C^* = T^*$, we obtain the following relations;

$$\Gamma = \tfrac{1}{2}$$

and (8)

$$T_C - T_C^* = 0.8 \text{ deg.}$$

Since near the transition temperature the correlation among molecules becomes strong, the short-range order may play some role in the thermal diffusion.

We obtained the same results for cholesteryl pelargonate, and they are shown in Figure 10. Compared with the case of MBBA, the critical region was narrow in this material. When discussing the cholesteric materials, de Gennes added another term to the free energy equation to account for the spatial gradient of the order parameter $Q$. The contribution of this term would make the difference between the nematic and the cholesteric materials.

We have shown the usefulness of high-speed optical holography for the dynamical study of the phase transition. In addition, we have observed an interesting phenomenon, namely, that sometimes the observed interference

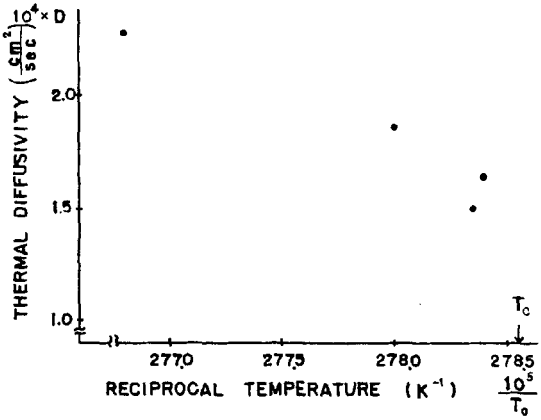


FIGURE 10 Temperature dependence of the diffusivity for Cholesteryl pelargonate. Temperature is expressed on the Kelvin scale.

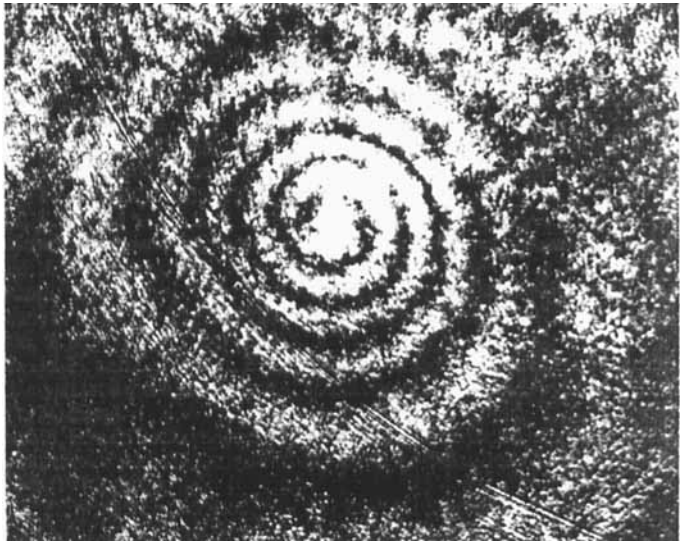

FIGURE 11 Reconstructed image from a double-exposed hologram. The observed interference fringes form a spiral.

fringes form a spiral. This is shown in Figure 11. The experimental condition for generation of the spiral refractive index line is not clear at present. We should take into consideration the effect of thickness of the sample cell. This is a further problem.

**Acknowledgement**

We wish to thank Dr K. Yoshimitsu for reading the manuscript. We are also indebted to Professor Clyde A. Hutchison Jr. of the University of Chicago for his helpful advice to improve the English in the text of the manuscript.



## Appendix

We examine the possibility of contribution of the short-range order parameter $\boldsymbol{Q}$ to the heat conductivity $K$. The equations concerning the density, the particle velocity and temperature fluctuations in a fluid are known as the hydrodynamic equations. In the case of the weak thermal fluctuations it is possible to very reliably linearize these hydrodynamic equations;

$$\frac{\partial \rho_1}{\partial t} + \rho_0(\nabla \cdot \mathbf{v}_1) = 0, \tag{A1}$$

$$\rho_0 \frac{\partial \mathbf{v}_1}{\partial t} + \frac{C_0^2}{\gamma} \nabla \rho_1 + \frac{\rho_0 \beta_0 C_0^2}{\gamma} \nabla T_1 - (\eta_0 \zeta) \nabla(\nabla \cdot \mathbf{v}_1) = 0, \tag{A2}$$

$$\rho_0 C_V \frac{\partial T_1}{\partial t} + \frac{\rho_0 C_V}{\beta_0} (\gamma - 1)(\nabla \cdot \mathbf{v}_1) - K_0 \nabla^2 T_1 = J, \tag{A3}$$

where $\rho_1$ is the density change, $\mathbf{v}_1$ is the velocity change, $T_1$ is the temperature change, $C_0$ is the sound speed, $\beta_0$ is the thermal expansion coefficient, $\gamma$ is the rate of specific heat, $\eta_0$ is viscosity, $\zeta$ is the viscosity number and $K_0$ is the thermal conductivity.

On the other hand, de Gennes has treated theoretically the flow birefringence of the isotropic phase in a liquid crystal. He has described the internal stress tensor by the linear combination of the shear rate tensor and the time derivative of $\boldsymbol{Q}$ tensor;

$$t_{ij} = b_1 e_{ij} + b_2 R_{ij}, \tag{A4}$$

where $t_{ij}$ is viscous stress tensor, $e_{ij}$ is the strain, $R_{ij}$ is $\partial Q_{ij}/\partial t$, $Q_{ij}$ is the tensor order parameter and $b_1$, $b_2$ are constants.

Both terms in the right hand side of Eq. A4 contribute to the velocity in the Navier-Stokes Eq. A2.

We take notice of the temperature region around the transition point. In this region it is probable that the second term of Eq. A4 becomes large. Furthermore, we make the experimental conditions so that we are able to neglect the effect of the macroscopic convection. Under these conditions the second term plays a dominant role.

Taking into consideration the contribution of Eq. A4 to Eq. A2, we represent the velocity in the approximate form;

$$\mathbf{v}_1 \simeq \frac{b_2}{\rho_0} \nabla Q_{ij}. \tag{A5}$$

Generally in the phase transition phenomena, the order parameter fluctuates remarkably at the transition point. We assume the temperature dependence of the fluctuation of $\boldsymbol{Q}$ in the following form;

$$\xi(T - T_C^*)^{-\Gamma},$$

where $\xi$ and $\Gamma$ are constants and $T_C^*$ is the characteristic temperature slightly different from $T_C$. Since our observation is limited to the fairly macroscopic size and observed patterns are axial symmetry, we regard $\xi$ as a scalar parameter which is the averaged value of $\boldsymbol{Q}$ over the appropriate volume. In addition, we assume that $T_0 - T_C^* \gg T_1$ ($T = T_0 + T_1$). The Laplacian of $\boldsymbol{Q}$ is approximately;

$$\nabla^2 \boldsymbol{Q} \simeq -\xi\Gamma(T_0 - T_C^*)^{-\Gamma-1} \nabla^2 T_1. \tag{A6}$$

From Eqs. A3, A5 and A6 we obtain

$$\rho_0 C_V \frac{\partial T_1}{\partial t} - K\nabla^2 T_1 = J, \tag{A7}$$

where

$$K = K_0 + \frac{C_V(\gamma - 1)b_2}{\beta_0} \xi\Gamma(T_0 - T_C^*)^{-\Gamma-1}. \tag{A8}$$

## References

1. T. W. Stinson and J. D. Litster, *Phys. Rev. Letters* **25**, 503 (1970).
2. T. W. Stinson and J. D. Litster, *J. Appl. Phys.* **41**, 996 (1970).
3. P. G. de Gennes, *Mol. Cryst. Liq. Cryst.* **12**, 193 (1971).
4. J. P. Gordon, *J. Appl. Phys.* **36**, 3 (1965).
5. J. Fisher and A. G. Fredrickson, *Mol. Cryst. Liq. Cryst.* **6**, 255 (1969).